Catalysis Today 261 (2016) 60–66

Contents lists available at ScienceDirect

Catalysis Today

journal homepage: www.elsevier.com/locate/cattod

Effects of noble metal promotion for Co/TiO_2 Fischer-Tropsch catalysts

Thomas O. Eschemann, Jogchum Oenema, Krijn P. de Jong*

Inorganic Chemistry and Catalysis, Debye Institute for Nanomaterial Science, Utrecht University, Universiteitsweg 99, 3584 CG Utrecht, P.O. Box 80083, 3508 TB Utrecht, The Netherlands

ARTICLE INFO

Article history:
Received 12 March 2015
Received in revised form 19 June 2015
Accepted 22 June 2015
Available online 13 August 2015

1. Introduction

The Fischer-Tropsch reaction involves the conversion of synthesis gas to higher hydrocarbons, which can then further be converted to ultraclean fuels or chemicals. While the synthesis gas can be derived from biomass, coal, or natural gas, the latter is the most economical option given current market prices and the availability of stranded gas and shale gas reserves. A crucial aspect for the economic viability for Fischer-Tropsch plants lies in the performance of the catalyst [1,2]. Because of their low water–gas shift activity, their high selectivity to higher hydrocarbons, and their stability, supported cobalt catalysts are preferred for plants processing synthesis gas derived from natural gas [3–7]. Supported cobalt catalysts used in industrial applications typically do not only contain 15–30 wt.% of catalytically active cobalt, but also 1–10 wt.% of metal oxides [8–11] and 0.1–1 wt. % of noble metals [8,12] in order to improve the activity, selectivity and stability of the catalysts [13].

While oxidic promoters are mainly used in order to ensure high selectivities to heavy products [8,12], noble metals are used to either improve the degree of reduction or the dispersion of supported cobalt catalysts. The addition of noble metals can shift the temperature needed to reduce cobalt oxide to metallic cobalt to distinctly lower temperatures, but its effect on the degree of reduction has been reported to be rather minor. Instead, the improved activity of noble metal promoted cobalt catalysts has been mainly attributed to higher cobalt dispersions [12,14–17], synergistic effects in the case of bimetallic particles [12,18–20], or the suppression of cobalt-support compound formation [12].

The activity of Fischer-Tropsch reaction has been found to linearly increase with the available metallic cobalt surface area, given constant turnover frequencies (TOF) [19]. This holds for catalysts with cobalt particles above a critical size of ~6 nm, below which the TOF drops sharply [21–23]. Above this critical size, the TOF has also been found to be independent of the support material used and noble metals present [12,16,19].

An exception on constant TOF has been reported earlier for the case of Ru-promoted Co/TiO_2 catalysts showing a three-fold higher surface-specific activity than unpromoted catalysts [18]. Similar results have also been found for Pt-promoted Co/Nb_2O_5 catalysts [24]. While in most cases studies on the impact of noble metal promotion on TOF were performed on Al_2O_3-supported catalysts, the support materials in the examples described above are reducible oxides that show strong metal support interactions towards group 8–10 metals, making them fundamentally different from other support materials typically used in Fischer-Tropsch catalyst preparation [25–27].

Here, we report on the structural and catalytic properties of noble metal promoted Co/TiO_2 catalysts prepared by co-impregnation with subsequent fluidized bed drying and heat treatment. Some of the most relevant noble metal promoters Ag, Pt, Ru, and Re were added in different atomic ratios. The heat-treated catalysts are characterized by TEM, XRD and TPR in order to obtain information on initial cobalt oxide dispersions and reducibility of the catalysts. Catalytic testing is carried out under industrial conditions in order to study the impact of noble metal addition on the catalytic properties. The spent catalysts are analyzed by TEM in order to calculate TOF during Fischer-Tropsch synthesis to answer the question whether the addition of noble metal promoters to cobalt supported on titania generally leads to higher intrinsic activity compared to unpromoted catalysts. *In situ* XRD studies are carried out in order to investigate whether the addition of noble metal promoters also influences the metallic cobalt phase formed during reduction, eventually determining the activity and selectivity during Fischer-Tropsch synthesis.

* Corresponding author. Tel.: +31 30 253 6762; fax: +31 30 251 1027.
E-mail address: k.p.dejong@uu.nl (K.P. de Jong).

http://dx.doi.org/10.1016/j.cattod.2015.06.016

2. Materials and methods

2.1. Catalyst synthesis

Noble metal promoted Co/TiO_2 catalysts were prepared by co-impregnation. Therefore, TiO_2 (Aeroxide P25, Evonik Degussa, pore volume 0.3 mL/g, BET surface area 50 m^2/g, 70% anatase, 30% rutile) was pre-sieved to 75–150 μm and dried under vacuum, before the support material was impregnated with an aqueous solution containing $Co(NO_3)_2{\cdot}6H_2O$ (4 M, Sigma-Aldrich, 99.99%) and one of the noble metal precursors $HRe(OH)_4$ (Sigma-Aldrich, 99.99%), $Ru(NO)(NO_3)_3$ (Sigma-Aldrich, 98.2%), $[(NH_3)_4Pt](NO_3)_2$ (Sigma-Aldrich, 99.995%) or $AgNO_3$ (Sigma-Aldrich, 99%) in concentrations to achieve atomic noble metal to cobalt ratios of 0.0035, 0.0070 and 0.0140. After that, the material was dried in a fluidized bed under a flow of N_2 at 353 K, before the heat treatment was carried out at 523 K (2 h, 2 K/min) in a fluidized bed under a flow of N_2. These catalysts are labeled Co XX NM YY, NM being the noble metal used, XX the cobalt weight loading (typically 9 wt.% assuming Co to be in the form of Co_3O_4) and YY the noble metal weight loading (0.05–0.39 wt.%). Unpromoted Co/TiO_2 catalysts were prepared analogously with a solution of $Co(NO_3)_2{\cdot}6H_2O$ (4 M, Sigma-Aldrich, 99.99%) and are labeled Co XX.

2.2. Catalyst characterization

X-ray powder diffraction (XRD) was performed on a Bruker D2 Phaser with a Co K_α (λ = 1.789 Å) source. Co_3O_4 crystallite size estimation was performed using the Co_3O_4 peak at 37° 2Θ with an automatic calculation routine in DiffracEvaluation V2.0 software by Bruker, which is based on the Debye-Scherrer-equation. Equivalent cobalt particle sizes are calculated from observed Co_3O_4 particle sizes by using the relation $d(\mathrm{Co}) = d(\mathrm{Co_3O_4}) \times 0.75$. Spent catalysts were found to be metallic cobalt covered with a thin wax layer, therefore no correction factor was applied.

For transmission electron microscopy (TEM), the heat-treated catalysts were ground with a mortar, suspended in ethanol using an ultrasonic bath and dropped onto a copper grid with holey carbon film. Spent catalysts were prepared in the same way. The samples were analyzed using a Tecnai T12 or a Tecnai T20 microscope, with electron beam voltage of 120 or 200 kV, respectively. While the support material consists of sharp-edges particles, the supported cobalt oxides particles could be identified by their rounded off shape. Equivalent cobalt particle sizes were calculated from observed Co_3O_4 particle sizes by using the relation $d(\mathrm{Co}) \times d(\mathrm{Co_3O_4}) \times 0.75$.

Temperature-programmed reduction (TPR) was carried out using a Micromeritics Autochem II ASAP 2920. Typically, 50 mg of the sample were dried in a flow of Ar at 373 K for 1 h and then reduced in a 50 N mL/min flow of H_2/Ar (1:19, v/v) at a temperature ramp of 5 K/min.

In situ X-ray powder diffraction studies were carried out on a Bruker D8 Phaser with a Co Kα (λ = 1.789 Å) source and equipped with an Anton Paar XRK reaction chamber. Typically, 50 mg of the powdered catalysts were dried under a flow of He and then reduced under a flow of H_2/He 1:3 (v/v) at 623 K (2 h, ramp 1 K/min).

2.3. Catalytic testing

Fischer-Tropsch synthesis was carried out in a 16 reactor catalytic testing setup (Flowrence, Avantium). The catalysts (75–150 μm) were diluted with SiC (200 μm) to a total bed volume of 200 μL in order to obtain desired CO conversion levels of 30%. The catalysts were dried in a flow of He for 2 h and then reduced *in situ* in a flow of H_2/He (1:3, v/v) at 623 K (8 h, ramp 1 K/min). Subsequently, the reactors were cooled to 453 K and pressurized to 20 bar under a flow of H_2. After switching to H_2/CO (2:1, v/v) the temperature was increased to 493 K (1 K/min). In the end of the experiment, most of the products remaining in the catalyst bed were removed under a flow of H_2 at 473 K, before the setup was cooled down to room temperature under a flow of He. The products were analyzed using online gas chromatography (Agilent 7890A), the permanent gases were separated on a Shincarbon column and quantified against He as an internal standard using a TCD detector. CO conversions were calculated as

$$X_{\mathrm{CO}} = \frac{(\mathrm{mol_{CO\,in}} - \mathrm{mol_{CO\,out}})}{\mathrm{mol_{CO\,in}}} \quad (1)$$

Hydrocarbons (C1–C9) were separated on a PPQ column, detected using an FID detector and quantified against the TCD signal of the internal standard He. Selectivities to the lower hydrocarbon fractions S_{CX} were calculated from converted CO and the corresponding yields as

$$S_{\mathrm{CX}} = \frac{Y_{\mathrm{CX}}}{\mathrm{mol_{CO\,in}} - \mathrm{mol_{CO\,out}}} \quad (2)$$

The selectivities to products with 5 and more carbon atoms are calculated from the yields to lower hydrocarbons as

$$S_{\mathrm{C5+}} = 1 - S_{\mathrm{C1-C4}} \quad (3)$$

CO conversion levels during the experiments were between 25% and 35%. Activities are reported as cobalt time yields (CTY, $\mathrm{mol_{CO}/(g_{Co}\,s)}$) and weight time yields (WTY, $\mathrm{mol_{CO}/(g_{Cat}\,s)}$). Turnover frequencies were calculated from TEM-derived surface average particle sizes, assuming full reduction to metallic cobalt based on literature [21], spherical geometries and a surface area of one cobalt atom of 0.0628 nm^2.

3. Results and discussion

The particle size analysis of the heat-treated catalyst precursors was carried out using TEM and XRD. (Fig. 1) The results showed very similar initial particle sizes of 4–7 nm for all promoted catalysts. Deviations between the measurement techniques can be explained by the fact of XRD analyzing crystallite sizes rather than particle sizes and being a bulk technique instead of a local imaging technique as TEM. For the unpromoted catalyst similarly sized cobalt oxide particle sizes were determined.

TEM imaging of the catalysts (Fig. 2) also revealed well-distributed supported cobalt oxide particles for unpromoted and promoted catalysts, which is in line with results previously reported. From TEM imaging no clear statement can be made on whether the cobalt oxide particles are doped with the noble metal promoters or whether the metals are present separately on the support material.

The reduction behavior of the promoted and unpromoted catalysts was studied using TPR (Fig. 3) The TPR results of the unpromoted Co/TiO_2 catalysts showed the typical two-step reduction pattern of Co_3O_4 to CoO (centered at 530 K) and CoO to Co (670 K). The use of Ag as a promoter was found to lead to a shift of both reduction peaks to lower temperatures, which was more pronounced in case of higher Ag loadings (500 and 600 K for the highest Ag loading), a trend previously reported for Ag-promoted Co/Al_2O_3 catalysts [17]. Promotion with different amounts of Pt led shifts of the reduction peaks to even lower temperatures (430 and 530 K for the highest Pt loading). It could be noted that already the lowest amount of Pt added led to a strong shift of the reduction peaks to lower temperatures (450 and 560 K), while the further shift with increasing Pt loadings was found to be less significant. These findings are in line with observations for Pt-promoted Co/Al_2O_3 catalysts previously reported [16,17]. Ru promotion also led to shifts in reduction temperature for both reduction steps. Largest shifts

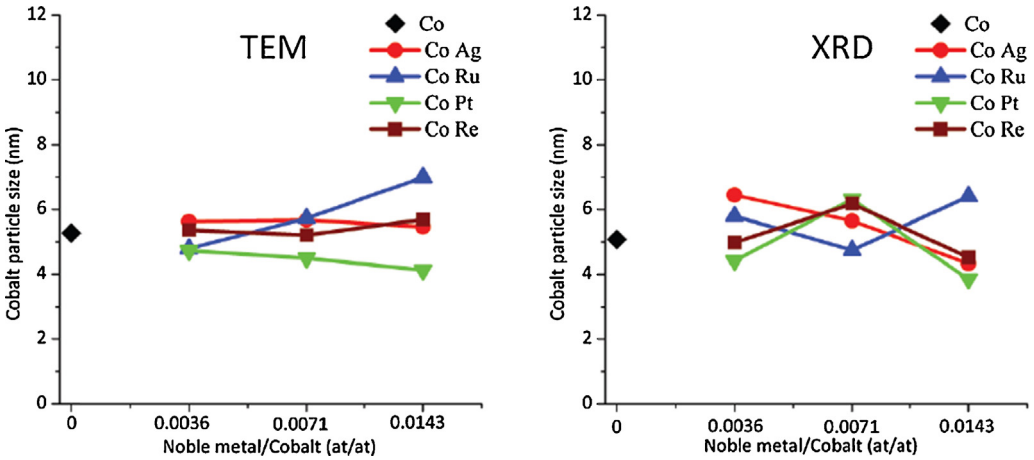

Fig. 1. Surface average equivalent cobalt particle sizes derived from TEM (left) and equivalent cobalt crystallite sizes derived from XRD line broadening analysis of the Co_3O_4 peak at 37° 2θ (right) of the heat-treated catalysts.

were found for the highest promoter loadings (450 and 560 K). For Re-promoted catalysts the first reduction peak was not affected for low and medium promoter loadings, while a shift to higher temperatures was observed for high Re loadings, an effect that has previously been attributed to the high reduction temperature of ReO_2 for the case of promoted Co/Al_2O_3 catalysts [16]. Only the second reduction peak was found to shift significantly to lower temperatures (620 K) As the initial cobalt oxide particle sizes were comparable for all catalysts, it can be assumed that all differences observed in the TPR patterns are due to the presence of the noble metal promoters and not dispersion effects [28]. A quantification of the TPR measurements in order to calculate the degree of reduction was not done because of the possibility of SMSI effects and its associated contribution to the TCD signal [29].

Fischer-Tropsch synthesis was carried out at 20 bar, 493 K and at very similar CO conversion levels. The results (Table 1) showed a cobalt time yield of 6.9 10^{-5} $mol_{CO}/(g_{Co}\ s)$ and a C_{5+}-selectivity of 85 wt.% for the unpromoted catalyst that are in good accordance with results published earlier [30,31]. The addition of Ag was also found to increase both activities ($10–12 \times 10^{-5}$ $mol_{CO}/(g_{Co}\ s)$) and the C_{5+} selectivity significantly to 87–89 wt.%. An increase of CTY was also found for the catalysts promoted with Pt, with an optimum found for the addition of 0.21 wt.% Pt. This activity gain was accompanied by decreased C_{5+} selectivities of only 82–84 wt.% that can partly be attributed to the hydrogenolysis and methanation activity of Pt. The addition of Ru also resulted in an increased activity, most pronounced for the addition of 0.10 wt.% Ru. Higher amounts of Ru were found to lead to higher C_{5+} selectivities. The addition of Re led to the most significant improvements in CTY and C_{5+} selectivity, comparable for all amounts of Re added.

In order to study the reasons for the different activities, the cobalt particle sizes of the spent catalysts were determined by TEM in order to calculate turnover frequencies. (Table 2) For the unpromoted catalysts, increased cobalt particle sizes were found after the catalytic testing and the TOF was in the expected range. For all catalysts promoted with Ag, bigger cobalt particles were found in the spent catalysts. While the effect of increasing cobalt dispersions is discussed for various noble metals [12,13], we only measure higher metal dispersions for Re-promoted catalysts. (Table 2, Fig. 4) The TOF of the catalysts promoted by Pt, Ru or Re were determined to be a factor of 2 higher than the TOF of the unpromoted catalyst, however, no strong influence of Ag was found. Pt promoted catalysts showed less average particle growth and TOF slightly lower than those of the Ag promoted catalysts. Neither CTY nor TOF of the Ag promoted catalysts were found to depend strongly on the promoter loading. Pt promoted catalysts showed increasing activities and TOF with increasing promoter loading initially, with lower values obtained for higher amounts of Pt. The cobalt particle sizes of the Ru promoted catalysts were found to be comparable with the other catalysts, but as for the CTY, a strong dependency of the amount of Ru added on the TOF was found. A medium Ru loading of 0.10 wt.% led to a three-fold TOF increase compared to the unpromoted catalyst. For the catalysts promoted with Re, cobalt particle sizes were found to be lower than the initial equivalent

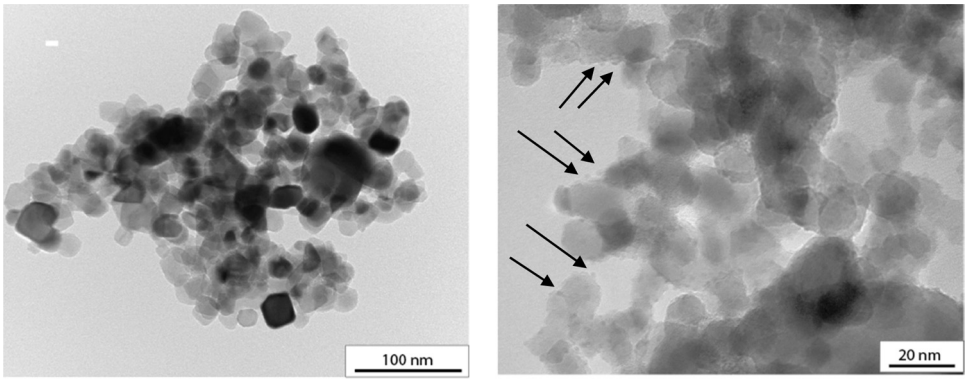

Fig. 2. TEM images of the unloaded TiO_2 P25 support material (left), and the TiO_2-supported Co catalyst, sample Co8.8Ag0.23 (right). Note the sharp edged titania support particles in the left, and the more rounded off shape of the supported cobalt oxide particles in the right image. The arrows indicate the position of a few supported cobalt oxide particles.

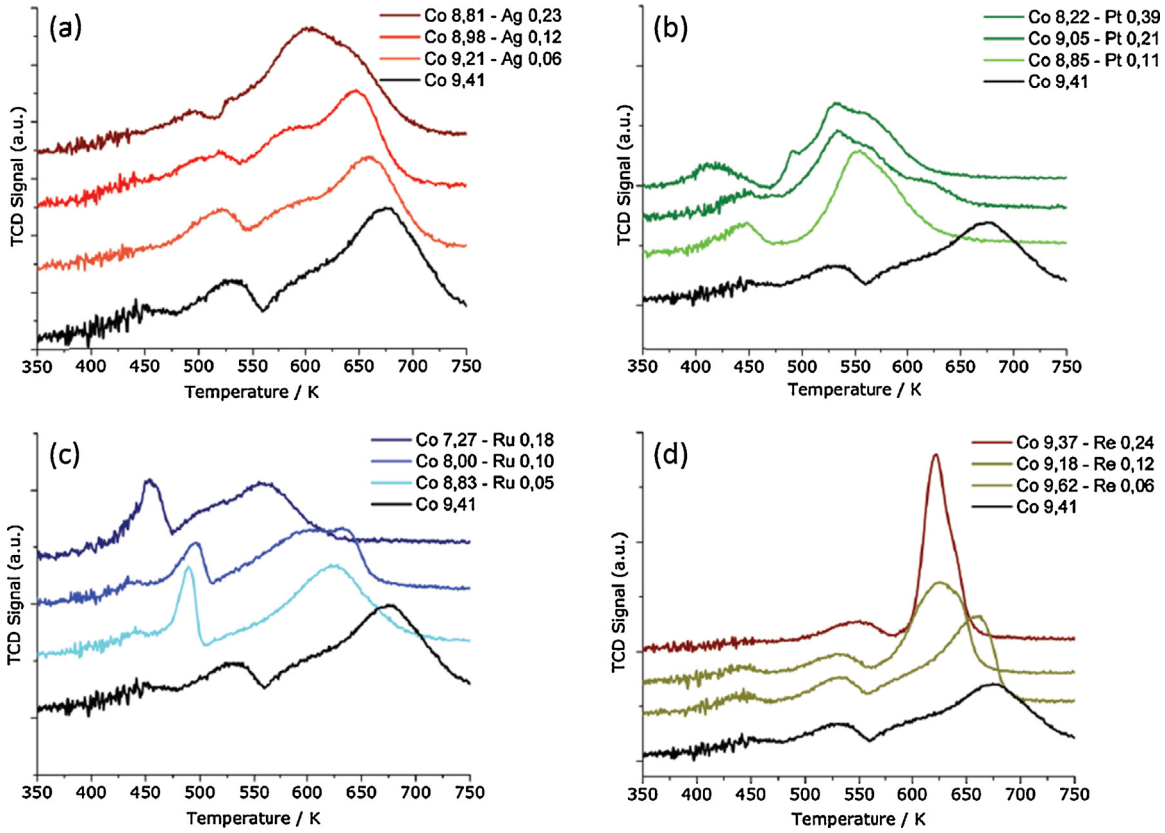

Fig. 3. TPR profiles for Ag-promoted (a), Pt-promoted (b), Ru-promoted and Re-promoted (d) Co/TiO_2 catalysts. For comparison the TPR profile of an unpromoted catalyst is given in black. The legends in all graphs provide the cobalt and noble metal loadings in wt.%.

cobalt particle sizes, which can be rationalized with the role of Re being a well-known dispersion enhancing noble metal promoter [12]. The TOF determined for these catalysts were around 0.04 s^{-1} for low and medium Re amounts and 0.06 s^{-1} for higher amounts of Re. These results suggest that for titania-supported cobalt catalysts a distinct increase in TOF can be observed upon the introduction of noble metal promoters, which is not observed for the addition of noble metal promoters on irreducible support materials [18]. It should be noted that possible differences in the degree of reduction were not considered in these calculations, although it has previously been reported that the degree of reduction for Co/TiO_2 catalysts is close to 100% and the effect of noble metal promotion on the degree of reduction is relatively small [16,31–34].

When discussing the degree of reduction of cobalt for these catalysts, the reducibility of the support material also needs to be considered. In the presence of supported metal nanoparticles, TiO_2 can be reduced to mobile TiO_x species, an effect that is known as strong metal support interaction (SMSI). These TiO_x species may then migrate and decorate the surface of the metal nanoparticles, thereby decreasing the accessible and catalytically active metal surface area. Given the characterization techniques utilized in this research, it remains unclear if and to which extent SMSI has taken place. Nevertheless, it should be considered that the nature and the amount of the noble metal promoter may influence the extent of SMSI and thereby the catalytic properties of the studied Co/TiO_2 catalysts.

Table 1
Catalytic performance of unpromoted and promoted Co/TiO_2 catalysts after 60 h of Fischer-Tropsch synthesis at 493 K, 20 bar, H_2/CO 2.0 (v/v).

	Catalyst	X_{CO} (%)	CTY/10^{-5} (mol_{CO}/g_{Co} s)	S_{CH4} (wt.%)	S_{C5+} (wt.%)
	Co 9.4	29.2	6.9	6.3	85
Ag-promoted	Co 9.2 Ag 0.06	30.3	10.0	6.5	89
	Co 9.0 Ag 0.12	33.9	11.9	6.4	89
	Co 8.8 Ag 0.26	33.1	10.5	7.0	87
Pt-promoted	Co 8.9 Pt 0.11	30.4	10.8	7.6	83
	Co 9.1 Pt 0.21	30.0	16.8	8.3	84
	Co 8.2 Pt 0.39	34.2	13.5	7.3	83
Ru-promoted	Co 8.8 Ru 0.05	26.4	7.2	6.9	82
	Co 8.0 Ru 0.10	30.3	14.5	9.3	84
	Co 7.3 Ru 0.18	31.8	13.5	7.0	88
Re-promoted	Co 9.6 Re 0.06	30.9	20.0	6.2	90
	Co 9.2 Re 0.13	26.7	18.6	6.7	88
	Co 9.4 Re 0.25	33.1	21.5	7.0	88

Table 2
Equivalent cobalt particle sizes of the fresh and spent unpromoted and promoted Co/TiO_2 catalysts and TOF after 60 h of Fischer-Tropsch synthesis at 493 K, 20 bar, H_2/CO 2.0 (v/v).

	Catalyst	d_{fresh} (nm)	d_{spent} (nm)	CTY/10^{-5} (mol_{CO} / g_{Co} s)	TOF_{spent} (s^{-1})
	Co 9.4	5.3	8.6	7.1	0.024
Ag-promoted	Co 9.2 Ag 0.06	5.6	11.8	10.0	0.066
	Co 9.0 Ag 0.12	5.7	10.3	11.9	0.068
	Co 8.8 Ag 0.26	5.8	10.1	10.5	0.059
Pt-promoted	Co 8.9 Pt 0.11	4.7	8.1	10.8	0.048
	Co 9.1 Pt 0.21	4.5	6.5	16.8	0.061
	Co 8.2 Pt 0.39	4.1	7.9	13.5	0.057
Ru-promoted	Co 8.8 Ru 0.05	5.5	8.1	7.2	0.032
	Co 8.0 Ru 0.10	5.7	10.5	14.5	0.084
	Co 7.3 Ru 0.18	7.0	7.8	13.5	0.057
Re-promoted	Co 9.6 Re 0.06	5.4	3.7	20.0	0.041
	Co 9.2 Re 0.13	5.2	3.7	18.6	0.039
	Co 9.4 Re 0.25	5.7	4.9	21.5	0.058

In order to obtain more information on the enhanced intrinsic activities of the promoted catalysts, *in situ* XRD studies were carried out, mimicking the reduction of the catalysts. (Fig. 5) The results revealed that for both unpromoted and promoted catalysts CoO was detected at 500 K. The CoO diffraction line disappeared at 623 K, while diffraction lines of metallic cobalt were found at this temperature. While for the unpromoted catalyst the peak was found to be at the expected diffraction angle for *fcc* Co, the peak was found to be broadened to higher diffraction angles for the Ag-promoted catalyst, probably indicating the presence of at least small amounts of *hcp* Co. It has been found previously that the formation of *hcp* cobalt leads to higher activities [35–37] and C_{5+} selectivities [38] during Fischer-Tropsch synthesis. It has also been shown that *hcp* Co is less prone to particle growth during Fischer-Tropsch synthesis than *fcc* Co [36]. Using *in situ* XRD, it has been demonstrated that this more active form can be formed by activation using synthesis gas [39] or by carbidization of cobalt oxide with subsequent reduction of CoC_2 to metallic Co [40]. The *hcp* structure is the thermodynamically stable phase below 723 K [1], although for particles below 20 nm the *fcc* structure is reported to prevail [41]. Nevertheless, the product typically formed upon reduction of Co_3O_4 particles under H_2 atmosphere at 623 K is *fcc* Co. Using TPR, we have demonstrated that the use of noble metal promoters leads to a shift of the reduction peaks to lower temperatures. It is thus suggested that an onset of the reduction at lower temperatures leads to the formation of *hcp* Co (partly) possibly contributing to the higher activities of the noble metal promoted catalysts. While in earlier studies stacking faults or the porosity of *hcp* cobalt were considered to explain the superior catalytic performance [35,37], recently DFT kinetic studies were carried out to shed light on the effect of the cobalt crystal structure on the elementary reaction steps of the Fischer-Tropsch reaction. It was demonstrated that CO activation proceeds with a higher rate

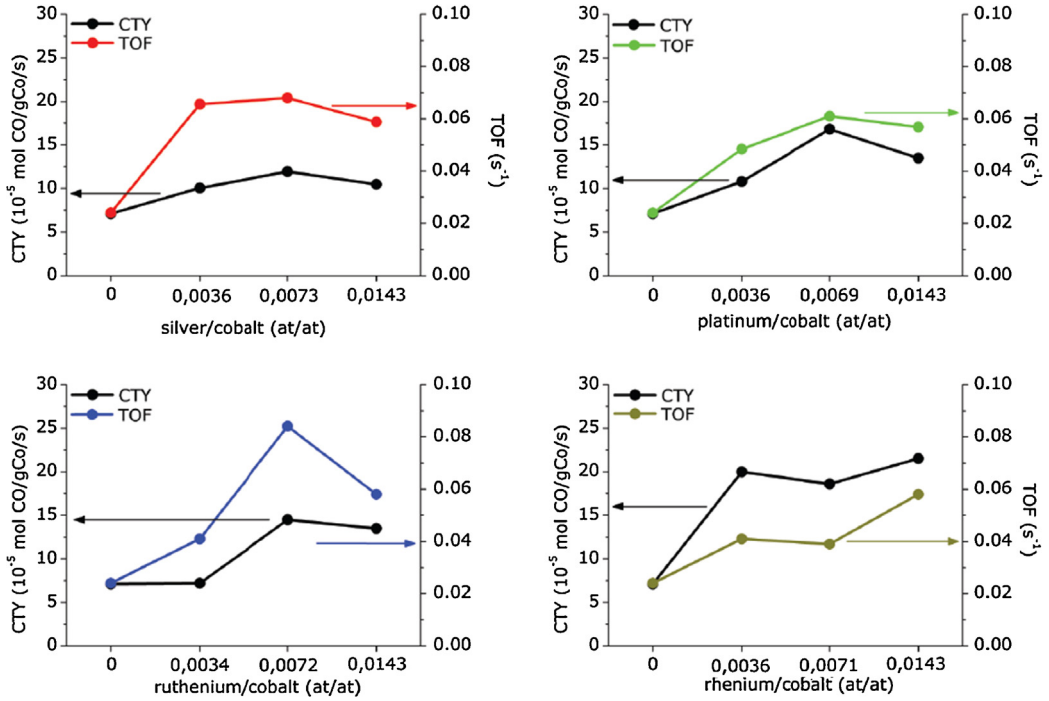

Fig. 4. TOF based on surface average TEM particle sizes of spent catalysts and CTY during Fischer-Tropsch synthesis at 493 K, 20 bar, H_2/CO 2.0 (v/v) for unpromoted and promoted catalysts.

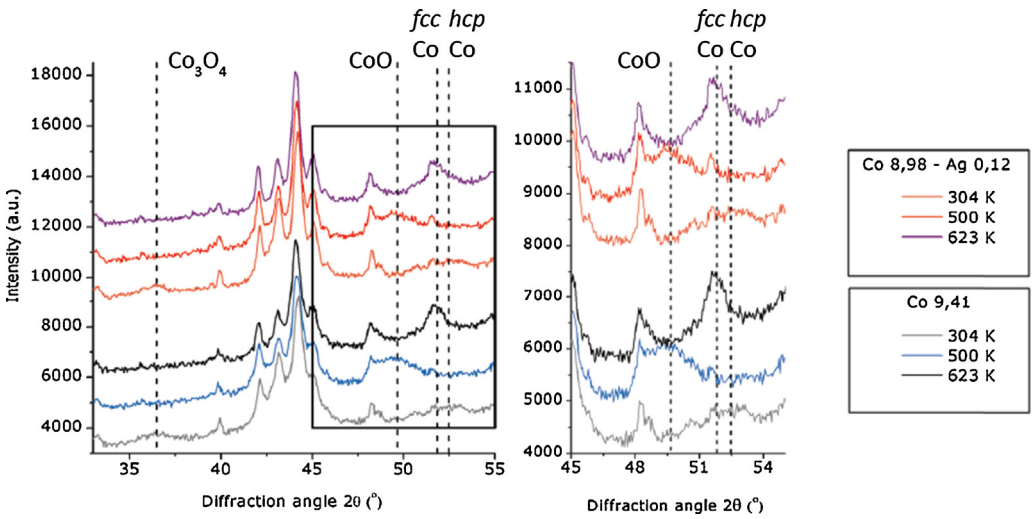

Fig. 5. *In situ* X-ray diffractograms for Ag-promoted and unpromoted Co/TiO_2 catalysts during and after reduction under a flow of H_2/He 1:3 (v/v).

on *hcp* Co, but also that it proceeds via direct dissociation, unlike H-assisted dissociation for *fcc* Co [42]. The role of the crystal structure of cobalt here can only be a first indication and should be addressed in future research, e.g. using on synchrotron-based *in situ* characterization techniques.

4. Conclusions and outlook

The XRD and TEM results showed that (co-)impregnation of TiO_2 with subsequent fluidized bed drying and heat treatment leads to a rather uniform distribution of similarly sized supported cobalt oxide particles for both unpromoted and promoted catalysts. TPR studies revealed that the addition of noble metals lead to decreased reduction temperatures of cobalt oxide, this effect being most pronounced for the addition of Pt and Ru and less pronounced for the addition of Re and Ag. The effect on the reduction temperature was found to increase with higher promoter loadings for all noble metals. The catalytic properties under industrial Fischer-Tropsch synthesis conditions were found to be strongly influenced by the addition of noble metals. While the addition of Ag, Re and higher amounts of Ru led to increased cobalt time yields and C_{5+}-selectivities, Pt-promoted catalysts showed only higher activities, but significantly lower C_{5+}-selectivities at very similar CO conversion. TEM studies of the reduced and spent catalysts showed that the cobalt particle sizes for the unpromoted and most promoted catalysts were similar, only Re-promoted catalysts showed distinctly lower particle sizes after the catalytic testing. TOF calculations based on the surface average TEM particle sizes of spent catalysts revealed that increased turnover frequencies were found for promoted catalysts as previously shown for Ru-promoted Co/TiO_2 and Pt-promoted Co/Nb_2O_5 catalysts [18,19,24], while the effect of TOF increase was most pronounced for Ru and Pt. Again, the influence of different degrees of reduction cannot be excluded from the calculations. *In situ* XRD studies revealed that for Ag-promoted catalysts, at least some *hcp* Co is formed, possibly contributing the higher intrinsic activities of these catalysts compared to the unpromoted system.

For Ru catalyzed Co/TiO_2, it was previously suggested that an interaction in bimetallic particles leads to reduced site blockage by carbonaceous species [18] or that the rate of surface oxygen and hydroxide removal was accelerated [19]. For Re-promoted catalysts, a close interaction of the promoter with the active metal was also discussed to rationalize the increased activities and selectivities [31]. Recent DFT studies [43] show that Co catalysts operate in a regime in which the overall reaction rate is controlled by CO dissociation and oxygen removal by water formation. It is widely accepted that the noble metals used as promoters are more active hydrogenation catalysts than cobalt [12], which can lead to synergistic effects in CO hydrogenation [44,45]. We suggest that increased hydrogenation activity in promoted catalysts accelerates water formation and/or gives rise to hydrogen-assisted CO dissociation [46–48].

Acknowledgements

We gratefully acknowledge Shell Global Solutions for financial support. We also thank Johan den Breejen, Heiko Oosterbeek and Sander van Bavel for fruitful discussions and Rien van Zwienen for technical assistance on high pressure catalytic testing. K.P.dJ. acknowledges support from an ERC Advanced Grant.

References

[1] A.Y. Khodakov, W. Chu, P. Fongarland, Chem. Rev. 107 (2007) 1692–1744.
[2] B.H. Davis, Cobalt FT catalysts, in: P.M. Maitlis, A. de Klerk (Eds.), Greener, 1st ed., Fischer-Tropsch Process. Fuels Feestocks, 2013, pp. 193–207.
[3] M.E. Dry, J. Chem. Technol. Biotechnol. 77 (2002) 43–50.
[4] M.E. Dry, Stud. Surf. Sci. Catal. 152 (2004) 533–600.
[5] M.E. Dry, Appl. Catal. A Gen. 189 (1999) 185–190.
[6] M.E. Dry, Appl. Catal. A Gen. 138 (1996) 319–344.
[7] J.L. Casci, C.M. Lok, M.D. Shannon, Catal. Today 145 (2009) 38–44.
[8] F. Morales, B.M. Weckhuysen, Promotion effects in Co-based Fischer-Tropsch catalysis, in: J.J. Spivey, K.M. Dooley (Eds.), Catalysis 19, The Royal Society of Chemistry, Cambridge, 2006, pp. 1–20.
[9] F. Morales, E. de Smit, F.M.F. de Groot, T. Visser, B.M. Weckhuysen, J. Catal. 246 (2007) 91–99.
[10] F. Morales, D. Grandjean, A. Mens, F.M.F. de Groot, B.M. Weckhuysen, J. Phys. Chem. B 110 (2006) 8626–8639.
[11] J.P. den Breejen, A.M. Frey, J. Yang, A. Holmen, M.M. van Schooneveld, F.M.F. de Groot, O. Stephan, J.H. Bitter, K.P. de Jong, Top. Catal. 54 (2011) 768–777.
[12] F. Diehl, A.Y. Khodakov, Oil Gas Sci. Technol. 64 (2009) 11–24.
[13] R. Oukaci, A.H. Singleton, J.G. Goodwin, Appl. Catal. A Gen. 186 (1999) 129–144.
[14] W. Chu, P. Chernavskii, L. Gengembre, G. Pankina, P. Fongarland, A.Y. Khodakov, J. Catal. 252 (2007) 215–230.
[15] G. Jacobs, W. Ma, P. Gao, B. Todic, T. Bhatelia, D.B. Bukur, B.H. Davis, Catal. Today 214 (2013) 100–139.
[16] G. Jacobs, T.K. Das, Y. Zhang, J. Li, G. Racoillet, B.H. Davis, Appl. Catal. A Gen. 233 (2002) 263–281.
[17] T. Jermwongratanachai, G. Jacobs, W. Ma, W.D. Shafer, M.K. Gnanamani, P. Gao, B. Kitiyanan, B.H. Davis, J.L.S. Klettlinger, C.H. Yen, D.C. Cronauer, J.A. Kropf, C.L. Marshall, Appl. Catal. A Gen. 464–465 (2013) 165–180.
[18] E. Iglesia, S.L. Soled, R.A. Fiato, H.V. Grayson, J. Catal. 143 (1993) 345–368.
[19] E. Iglesia, Appl. Catal. A Gen. 161 (1997) 59–78.
[20] E. Iglesia, S.L. Soled, R.A. Fiato, J. Catal. 137 (1992) 212–224.

[21] J.P. den Breejen, P.B. Radstake, G.L. Bezemer, J.H. Bitter, V. Frøseth, A. Holmen, K.P. de Jong, J. Am. Chem. Soc. 131 (2009) 7197–7203.
[22] J.P. den Breejen, J.R.A. Sietsma, H. Friedrich, J.H. Bitter, K.P. de Jong, J. Catal. 270 (2010) 146–152.
[23] G.L. Bezemer, J.H. Bitter, H.P.C.E. Kuipers, H. Oosterbeek, J.E. Holewijn, X. Xu, F. Kapteijn, A.J. van Dillen, K.P. de Jong, J. Am. Chem. Soc. 128 (2006) 3956–3964.
[24] J.H. den Otter, K.P. de Jong, Top. Catal. 57 (2013) 445–450.
[25] S.J. Tauster, S.C. Fung, R.L. Garten, J. Am. Chem. Soc. 100 (1978) 170–175.
[26] S.J. Tauster, Acc. Chem. Res. 20 (1987) 389–394.
[27] F.M.T. Mendes, A. Uhl, D.E. Starr, S. Guimond, M. Schmal, H. Kuhlenbeck, S.K. Shaikhutdinov, H.-J. Freund, Catal. Lett. 111 (2006) 35–41.
[28] A.M. Saib, A. Borgna, J. van de Loosdrecht, P.J. van Berge, J.W. Geus, J.W. Niemantsverdriet, J. Catal. 239 (2006) 326–339.
[29] M. Voß, D. Borgmann, G. Wedler, J. Catal. 212 (2002) 10–21.
[30] T.O. Eschemann, J.H. Bitter, K.P. de Jong, Catal. Today 228 (2014) 89–95.
[31] S. Storsæter, B. Tøtdal, J.C. Walmsley, B.S. Tanem, A. Holmen, J. Catal. 236 (2005) 139–152.
[32] J. Li, G. Jacobs, T. Das, B.H. Davis, Appl. Catal. A Gen. 233 (2002) 255–262.
[33] B. Jongsomjit, C. Sakdamnuson, J. Panpranot, P. Praserthdam, React. Kinet. Catal. Lett. 88 (2006) 65–71.
[34] A. Michalak, M. Nowosielska, W.K. Jóźwiak, Top. Catal. 52 (2009) 1044–1050.
[35] O. Ducreux, B. Rebours, J. Lynch, D. Bazin, Oil Gas Sci. Technol. 64 (2009) 49–62.
[36] H. Karaca, O.V. Safonova, S. Chambrey, P. Fongarland, P. Roussel, A. Griboval-Constant, M. Lacroix, A.Y. Khodakov, J. Catal. 277 (2011) 14–26.
[37] M. Sadeqzadeh, H. Karaca, O.V. Safonova, P. Fongarland, S. Chambrey, P. Roussel, A. Griboval-Constant, M. Lacroix, D. Curulla-Ferré, F. Luck, A.Y. Khodakov, Catal. Today 164 (2011) 62–67.
[38] M.K. Gnanamani, G. Jacobs, W.D. Shafer, B.H. Davis, Catal. Today 215 (2013) 13–17.
[39] O'Shea. V a de la Peña, N. Homs, J.L.G. Fierro, P. Ramírez de la Piscina, Catal. Today 114 (2006) 422–427.
[40] L. Braconnier, E. Landrivon, I. Clémençon, C. Legens, F. Diehl, Y. Schuurman, Catal. Today 215 (2013) 18–23.
[41] O. Kitakami, H. Sato, Y. Shimada, F. Sato, M. Tanaka, Phys. Rev. B 56 (1997) 13849–13854.
[42] J.-X. Liu, H.-Y. Su, D.-P. Sun, B.-Y. Zhang, W.-X. Li, J. Am. Chem. Soc. 135 (2013) 16284–16287.
[43] I.A.W. Filot, R.A. Van Santen, E.J.M. Hensen, Angew. Chem. Int. Ed. Engl. 53 (2014) 12746–12750.
[44] L. Guczi, L. Borkó, Z. Schay, D. Bazin, F. Mizukami, 65 (2001) 51-57.
[45] Z.S.L. Guczi, G. Stefler, F. Mizukami, J. Mol. Catal. A Chem. 141 (1999) 177–185.
[46] J. Yang, Y. Qi, J. Zhu, Y.A. Zhu, D. Chen, A. Holmen, J. Catal. 308 (2013) 37–49.
[47] M.R. Elahifard, M.P. Jigato, J.W. Niemantsverdriet, ChemPhysChem 13 (2012) 89–91.
[48] S. Shetty, A.P.J. Jansen, R.A. van Santen, J. Am. Chem. Soc. 131 (2009) 12874–12875.